INSTITUTE OF PHYSICS PUBLISHING JOURNAL OF PHYSICS: CONDENSED MATTER

J. Phys.: Condens. Matter **18** (2006) 3745–3752 doi:10.1088/0953-8984/18/15/019

Structure and magnetic properties of hollandite $Ba_{1.2}Mn_8O_{16}$

S Ishiwata[1,2], J W G Bos[1], Q Huang[3] and R J Cava[1]

[1] Department of Chemistry, Princeton University, Princeton, NJ 08544, USA
[2] Department of Applied Physics, Waseda University, Ookubo, Shinjuku, Tokyo 169-8555, Japan
[3] NIST Center for Neutron Research, National Institute of Standards and Technology, Gaithersburg, MD 20899, USA

E-mail: ishiwata@htsc.sci.waseda.ac.jp

Received 21 December 2005
Published 30 March 2006
Online at stacks.iop.org/JPhysCM/18/3745

Abstract

The synthesis, crystal structure and magnetic properties of $Ba_{1.2}Mn_8O_{16}$, obtained using a KCl mineralizer, are reported. This material crystallizes in the monoclinic hollandite structure, containing Mn–O double chains (space group: $I2/m$, $a = 10.052(1)$ Å, $b = 2.8579(2)$ Å, $c = 9.7627(10)$ Å, $\beta = 89.96(1)^\circ$), and undergoes a magnetic transition at 40 K with the magnetization having a small ferromagnetic component. The ordering temperature is nearly 10 times lower than expected from the Weiss temperature of −385 K, evidencing magnetic frustration. Preliminary neutron powder diffraction studies suggest a complex spin arrangement within the ac-plane (perpendicular to the chain axis). The resistivity is consistent with one-dimensional variable range hopping.

1. Introduction

Competition between magnetic ground states can often be the source of unexpected electronic phenomena when the system is perturbed by an applied magnetic or electric field. Manganese oxides having the $AMnO_3$ (A = La, Sr, etc) perovskite structure satisfy this criterion [1, 2]. They typify strongly correlated electron systems where the interplay between spin, charge, orbital, and lattice degrees of freedom plays a crucial role in determining the physical properties. Through tuning the Mn–O–Mn bond angle and the oxidation state of Mn ions between 3+ and 4+, they can be made to display various ground states, such as antiferromagnetic charge/orbital-ordered insulator or ferromagnetic metal. Due to the competition between these phases, applying external magnetic fields near a critical temperature and composition causes a drastic change in resistivity—called the colossal magnetoresistance effect [3, 4]. Changing structural dimensionality is also an important strategy for improving magnetoelectronic performance. Layered manganese oxides with Ruddlesden–Popper structure, $A_{n+1}Mn_nO_{3n+1}$ (e.g. A = La, Sr; $n = 1, 2, \ldots$) [5],

are considered to be natural spin-valve systems, where spin-polarized metallic layers are sandwiching insulating antiferromagnetic layers [6].

Although hollandite-type manganese oxides, $A_xMn_8O_{16}$ (A = K, Ba, Pb, etc), with 1D tunnel structures have been under extensive investigation for applications as, e.g., ionic conductors, positive electrodes, and oxidation catalysts, less attention has been paid to their magnetic and electronic properties [7–9]. This may be because hollandite materials are prepared typically through soft chemistry resulting in poor crystallinity. Recently, some hollandite oxides, containing for example ruthenium, $Ba_{1.33}Ru_8O_{16}$ ($BaRu_6O_{12}$) [10], and vanadium, $Bi_xV_8O_{16}$ ($1.6 \leqslant x \leqslant 1.8$) [11], were found to show anomalous electronic properties inherent to the quasi-one-dimensional double chains of MO_6 (M = Ru or V) octahedra. Low dimensionality, promoting quantum spin fluctuations or geometric frustration, has been proposed as the origin of these electronic properties. We have therefore examined a manganese hollandite, $Ba_xMn_8O_{16}$, in order to explore the possibility of finding novel magnetic phases in the non-perovskite manganese oxides.

We report here the magnetic properties of the monoclinic hollandite, $Ba_{1.2}Mn_8O_{16}$, prepared by solid state reaction. Crystal structure, electrical resistivity, and preliminary neutron scattering data are also described.

2. Experiment

Polycrystalline samples of $Ba_{1.2}Mn_8O_{16}$ were prepared by solid state reaction. A mixture of $Ba(NO_3)_2$, Mn_2O_3, and KCl in a molar ratio of 1.2:4:12 was ground thoroughly in an agate mortar (0.5–1 h) and pressed into pellets. The pellets were heated in a covered alumina crucible slowly (100 °C h^{-1}) up to 850 °C, soaked for 72 h, and then heated at 900 °C for 48 h in air with an intermediate grinding. A KCl mineralizer was found to be necessary to facilitate the formation of the hollandite phase over the formation of the perovskite phase $BaMnO_3$. Attempts to obtain single-phase $Ba_xMn_8O_{16}$ with $x \leqslant 1.1$ and $x \geqslant 1.3$ were unsuccessful; the former gave a mixture of the hollandite phase and Mn_2O_3, while the latter contained a small amount of $BaMnO_3$ or $Ba_6Mn_{24}O_{48}$ as an impurity [12]. The samples obtained were washed in distilled water to dissolve KCl and dried at 100 °C. To measure resistivity, powder from a washed sample was pressed into a dense pellet and sintered at 900 °C for 24 h.

Powder XRD data at room temperature were recorded at a 0.02° step size with a Bruker D8 diffractometer using Cu Kα radiation and a diffracted beam monochromator[4]. The data were analysed by the Rietveld method using the program GSAS on the basis of space group $I2/m$ (No 12, the third choice for $C2/m$) [13]. The occupancies of the Mn and oxygen sites were found to be stoichiometric, and therefore were fixed to 1 during the final refinements. Neutron diffraction data for characterizing the magnetic ordering were collected using the BT-1 high resolution powder neutron diffractometer at the NIST Center for Neutron Research, employing a Cu(311) monochromator to produce a neutron beam of wavelength 1.5403 Å. Collimators with horizontal divergences of 15′, 20′, and 7′ of arc were used before and after the monochromator, and after the sample, respectively.

DC magnetic susceptibility measurements were measured with a Quantum Design MPMS SQUID magnetometer in external magnetic fields of 0.01, 0.1, and 1 T. The AC magnetic susceptibility and four-probe electrical resistivity measurements were performed with a Quantum Design PPMS.

[4] Certain commercial products and equipment are identified in this report to describe the subject adequately. Such identification does not imply recommendation or endorsement by the NIST, nor does it imply that the equipment identified is necessarily the best available for the purpose.

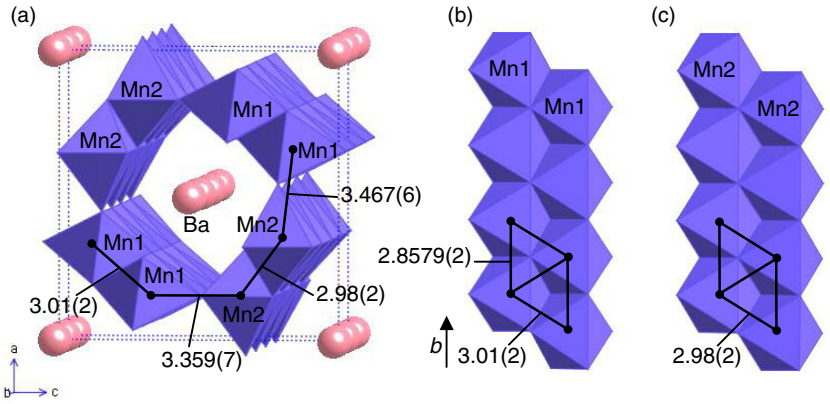

Figure 1. (a) The crystal structure of $Ba_{1.2}Mn_8O_{16}$. ((b), (c)) The linkage of the double chains viewed perpendicular to the *b*-axis. Selected Mn–Mn distances are shown.

(This figure is in colour only in the electronic version)

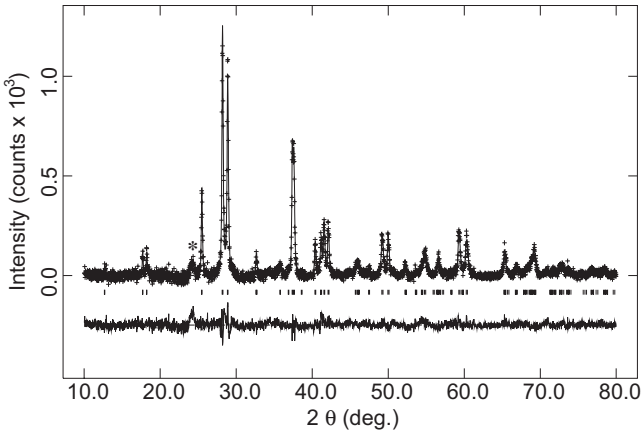

Figure 2. Observed (+), calculated (solid line), and difference x-ray powder diffraction (Cu Kα) Rietveld profiles for $Ba_{1.2}Mn_8O_{16}$. The tick marks indicate the calculated peak positions. The peak marked with the asterisk has not been identified.

3. Results and discussion

The structure of $Ba_{1.2}Mn_8O_{16}$ consists of pseudo-orthorhombic $[Mn_8O_{16}]_n$ tunnels in which the Ba ions are distributed (figure 1(a)). The tunnels consist of double chains of edge-sharing MnO_6 octahedra, linked by corners to each other. The Mn–Mn network forms an isosceles triangular lattice within the double chains (figures 1(b), (c)). The powder XRD pattern of $Ba_{1.2}Mn_8O_{16}$, shown in figure 2, was indexed with a monoclinic cell ($a = 10.052(1)$ Å, $b = 2.8579(2)$ Å, $c = 9.7627(10)$, $\beta = 89.96(1)°$). Note that the monoclinic angle is quite close to 90°, whereas the previous reports for $BaMn_8O_{16}$ and $Ba_2Mn_8O_{16}$, which are minerals, have a larger monoclinic angle (91°–91.2°) [14, 15]. The atomic positions, selected bond distances, and bond angles are listed in tables 1–3, respectively. Diffusion of Ba ions in the tunnels may result in the anomalously large thermal parameter $B = 3.3$ Å^2. The refined occupancy of the Ba site, 0.313(4), is close to the value for the nominal composition, 0.3. It should be noted that

Table 1. Occupancies, atomic positions, and atomic displacement parameters for $Ba_{1.2}Mn_8O_{16}$.

Atom	Site	Occupancy	x	y	z	B (Å^2)
Ba1	4g	0.313(4)	0	0.382(4)	0	3.3(5)
Mn1	4i	1	0.161(1)	0	0.350(1)	0.37(2)
Mn2	4i	1	0.347(1)	0	0.839(1)	0.37(2)
O1	4i	1	0.198(2)	0	0.152(2)	0.37(2)
O2	4i	1	0.162(3)	0	0.795(2)	0.37(2)
O3	4i	1	0.161(2)	0	0.542(3)	0.37(2)
O4	4i	1	0.550(2)	0	0.814(2)	0.37(2)

$a = 10.052(1)$ Å, $b = 2.8579(2)$ Å, $c = 9.7627(10)$ Å, $\beta = 89.96(1)°$, $Z = 1$, $V = 280.47(7)$ Å^3, $R_{wp} = 9.33\%$, $R_p = 7.34\%$, $\chi^2 = 1.55$.

Table 2. Selected Mn–O bond lengths for $Ba_{1.2}Mn_8O_{16}$.

Atoms	Bond length (Å)
Mn1–O1	2.01(2)(×2)
	1.97(3)
Mn1–O3	1.88(3)
Mn1–O4	1.85(1)(×2)
Mn2–O2	1.94(2)(×2)
	1.91(2)
Mn2–O3	1.84(2)(×2)
Mn2–O4	2.05(2)

Table 3. Selected Mn–O–Mn bond angles for $Ba_{1.2}Mn_8O_{16}$.

Atoms	Bond angle (deg)
Mn1–O1–Mn1	98(1) (×2)
	90(1)
Mn1–O4–Mn1	101(1)
Mn2–O2–Mn2	101(1) (×2)
	95(1)
Mn2–O3–Mn2	102(1)
Mn1–O3–Mn2	129(1)(×2)
Mn1–O4–Mn2	125(1)(×2)

syntheses in oxygen flow gave essentially the same compound, at least as examined through XRD and magnetic studies, which means that the oxygen sites are fully occupied and rather robust in this hollandite structure. With no oxygen deficiency in the present material, the formal oxidation state of the Mn ions is near 3.7+. Consistent with this, the average Mn–O bond length (1.92 Å) is close to that of the 2H perovskite $BaMn^{4+}O_3$ (1.90 Å) [16] but much smaller than that observed for $LaMn^{3+}O_3$ (2.02 Å) [17]. It is of interest that the MnO_6 octahedra are rather distorted (see table 2). An electronic band structure calculation may be of future interest for elucidating the origin of the distortion.

Figure 3 shows the temperature dependence of the magnetic susceptibility for $Ba_{1.2}Mn_8O_{16}$ for field cooling (FC) and zero-field cooling (ZFC). A small hump, indicating a magnetic transition, was observed, with an onset of 40 K. We interpret this as being due to magnetic ordering ($T_m = 40$ K). The data between 150 and 300 K were fitted to the Curie–Weiss law with a temperature independent term, $\chi(T) = \chi_0 + C/(T - \theta)$, $\chi_0 = 2.62 \times 10^{-5}$ emu Oe^{-1}/mol Mn, $C = 2.11$ emu K Oe^{-1}/mol Mn, and $\theta = -385$ K. The estimated

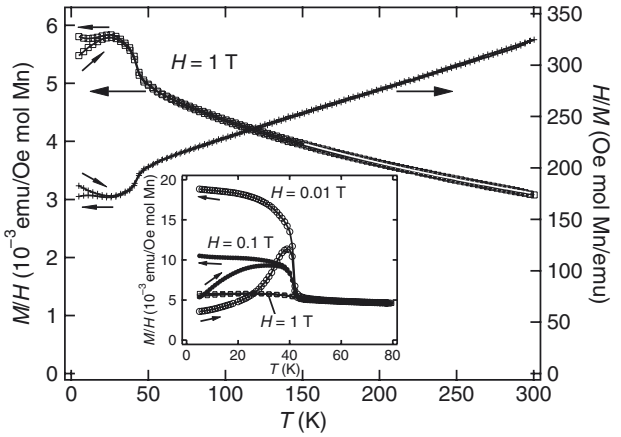

Figure 3. Temperature dependence of magnetic susceptibility and inverse magnetic susceptibility for $Ba_{1.2}Mn_8O_{16}$ measured in a magnetic field of 1 T. The Curie–Weiss fit is also shown. Data measured in magnetic fields of 0.01, 0.1, and 1 T over a narrow temperature range are shown in the inset.

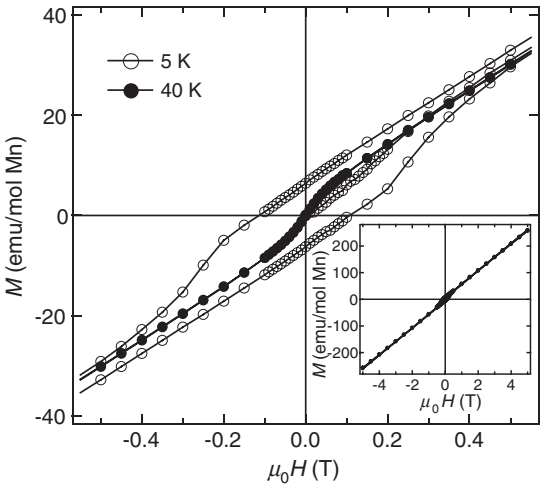

Figure 4. Magnetization curves of $Ba_{1.2}Mn_8O_{16}$ at 5 and 40 K, measured from zero-field cooling in an applied field, $0 \rightarrow 5 \rightarrow -5 \rightarrow 5$ T. The inset shows the whole plot.

effective moment per Mn mole ($P_{\text{eff}} = 4.11\ \mu_B$) is quite close to the expected value ($P_{\text{calc}} = 4.18\ \mu_B$) assuming a high spin state for Mn, and a mixture of Mn^{3+} and Mn^{4+} with an average valence 3.7+. Strong antiferromagnetic interactions are indicated by the large negative Weiss constant, θ, whose magnitude is almost ten times larger than the ordering temperature, T_m. The presence of a ferromagnetic contribution to the magnetization was seen below the ordering temperature when measuring magnetic susceptibilities under lower magnetic fields (0.1 and 0.01 T). A magnetic hysteresis loop opens below T_m, and the coercive field increases as temperature decreases (figure 4). Although the magnetic state below 40 K is fundamentally antiferromagnetic in character, seen through a magnetization that primarily increases linearly as a function of magnetic field, there is a small ferromagnetic component, perhaps due to tilting of the ordered spins within the low symmetry structure.

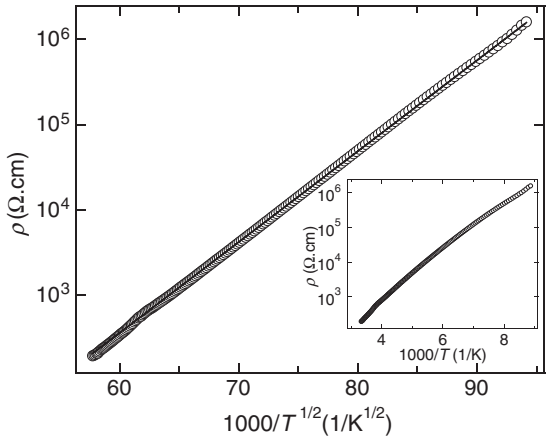

Figure 5. The linear fitting of $\log \rho$ versus $1/T^{1/2}$. The inset shows the Arrhenius plot for $\log \rho$ versus $1/T$. The data were collected on cooling at a rate of 2 K min^{-1}.

The temperature dependence of the resistivity is shown in figure 5. The linear plot in the main panel indicates that the dominant conduction mechanism is one-dimensional variable range hopping (VRH) rather than thermal activation-type over this temperature range (115–300 K). The formula for VRH conduction is expressed as

$$\rho(T) = \rho(T_0) \exp(T_0/T)^{1/(d+1)}, \tag{1}$$

where T_0 is a characteristic temperature and d is the dimensionality of the system [18]. Fits with $d = 2$ and 3 were less successful. This result is a hallmark of the one-dimensional electronic character of $Ba_{1.2}Mn_8O_{16}$, and is possibly affected by the short ranged incommensurate ordering of Ba ions [19]. Such incommensurate structures are often found in hollandite oxides $A_xM_8O_{16}$ (A = K, Ba; M = 3d transition metal; $1 \leqslant x \leqslant 2$) [20]. These data indicate that the double-exchange mechanism known to induce itinerant ferromagnetism in the perovskites is absent in the present case: as the resistivity at low temperatures is quite high, the electrons should be almost localized at temperatures in the vicinity of the magnetic transition. Consistent with this, no significant magnetoresistance was observed.

In figure 6, the neutron powder diffraction patterns of $Ba_{1.2}Mn_8O_{16}$ above and below the magnetic ordering temperature (∼40 K) are shown. The extra Bragg reflections observed at 4 K (more visible in the difference plot) indicate the presence of long range magnetic ordering. They are indexed with a (1/2 0 1/2) superlattice. Sato *et al* have proposed a helical spin structure with a propagation vector along the chain axis in a hollandite, $K_{1.5}(H_3O)_xMn_8O_{16}$, with tetragonal $I4/m$ symmetry at room temperature [19]. However, the magnetic unit cell of $Ba_{1.2}Mn_8O_{16}$ is enlarged twice in the a- and c-directions, excluding the possibility of a similar helical spin structure. The complex interaction between the chains may lead to a doubling of the unit cell within the ac-plane. As the magnetic Bragg peaks are much broader than the nuclear peaks, the ordered magnetic domain size is smaller than the crystalline size of the sample for the nuclear structure.

Finally, we comment on the origin of the magnetic behaviour in the present material. Two possible factors could result in the rather low T_m compared to the Weiss temperature. One possibility is geometrical frustration. As shown in figure 1(b), the Mn–Mn network forms a triangular lattice that, supposing all interactions are antiferromagnetic, should suppress the ordering. In addition, Mn^{4+} is expected to be spherical, which is favourable to

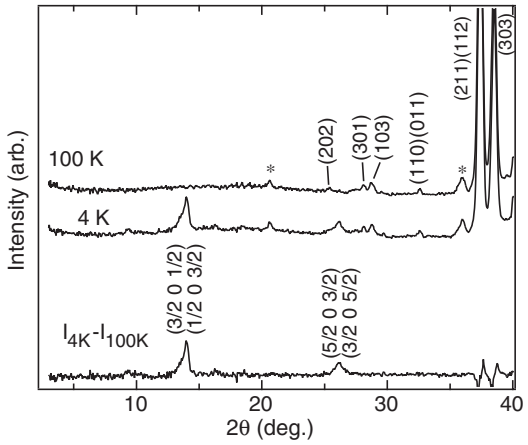

Figure 6. Neutron diffraction profiles at 100, 4 K, and the difference plot. The magnetic Bragg reflections are indexed assuming a superlattice, (1/2 0 1/2). The structural Bragg reflections at 100 K and the magnetic Bragg reflections in the difference plot are indexed. The peaks marked with asterisks have not been identified.

geometrical frustration. The other possibility is magnetic frustration caused by the competition between ferromagnetic and antiferromagnetic interactions. According to the Kanamori–Goodenough rule, the superexchange interaction in Mn–O–Mn varies from antiferromagnetic to ferromagnetic as the Mn–O–Mn bond angle decreases from 180° to 90° [21, 22]. Indeed, as seen in table 3, some of the Mn–O–Mn bond angles of $Ba_{1.2}Mn_8O_{16}$ are quite close to 90° (90°–95°) and others are on the verge of reversal of the exchange interaction (98°–129°). Although local distortions or disorder may cause magnetic frustration, that is unlikely in the present case because it typically leads to spin glass behaviour, which is inconsistent with the results of our preliminary neutron diffraction study and the character of the measured magnetic susceptibility.

4. Conclusions

In summary, we have characterized the structure and magnetic properties of a hollandite, $Ba_{1.2}Mn_8O_{16}$. The refined occupancy of Ba ions, Mn–O bond distances, and the Curie–Weiss fit for the paramagnetic susceptibility are consistent with the nominal composition. This compound undergoes a magnetic transition at 40 K (T_m) with the magnetization having a small ferromagnetic component. The T_m being significantly lower than the Weiss temperature of −385 K signals the presence of magnetic frustration due to the presence of structural triangles or competing ferromagnetic and antiferromagnetic interactions, or suppressed T_m due to the low dimensionality of the structure. The dominant conduction mechanism is one-dimensional variable range hopping, and the electrons are localized at low temperatures. Detailed neutron diffraction and electron microscope studies to elucidate the magnetic structure and the presence of charge ordering are worth future consideration.

Acknowledgments

This work was supported by the Japan Society for the Promotion of Science, and by the US National Science Foundation, grant NSF DMR 0244254.

References

[1] Ramirez A P 1997 *J. Phys.: Condens. Matter* **9** 8171
[2] Hotta T and Dagotto E 2000 *Phys. Rev.* B **61** 11879
[3] Tomioka Y, Asamitsu A, Moritomo Y, Kuwahara H and Tokura Y 1995 *Phys. Rev. Lett.* **74** 5108
[4] Murakami S and Nagaosa N 2003 *Phys. Rev. Lett.* **90** 197201
[5] Ruddlesden S N and Popper P 1951 *Acta Crystallogr.* **10** 538
[6] Kimura T, Tomioka Y, Kuwahara H, Asamitsu A, Tamura M and Tokura Y 1996 *Science* **274** 1698
[7] Brock S L, Duan N G, Tian Z R, Giraldo O, Zhou H and Suib S L 1998 *Chem. Mater.* **10** 2619
[8] Feng Q, Horiuchi T, Mitsusio T, Yanagisawa K and Yamasaki N 1999 *J. Mater. Sci. Lett.* **18** 1375
[9] Barbato S and Gautier J L 2001 *Electrochim. Acta* **46** 2767
[10] Mao Z Q, He T, Rosario M M, Nelson K D, Okuno D, Ueland B, Deac I G, Schiffer P, Liu Y and Cava R J 2003 *Phys. Rev. Lett.* **90** 186601
[11] Waki T, Kato H, Kato M and Yoshimura K 2004 *J. Phys. Soc. Japan* **73** 275
[12] Boullay P, Hervieu M and Raveau B 1997 *J. Solid State Chem.* **132** 239
[13] Larson A and VonDreele R B 1994 *Los Alamos National Laboratory, Internal Report*
[14] Nistor L C, Van Tendeloo G and Amelinckx S 1994 *J. Solid State Chem.* **109** 152
[15] Miura H 1986 *Mineral. J.* **13** 119
[16] Cussen E J and Battle P D 2000 *Chem. Mater.* **12** 831
[17] Huang Q, Santoro A, Lynn J W, Erwin R W, Borchers J A, Peng J L and Greene R L 1997 *Phys. Rev.* B **55** 14987
[18] Itkis M E, Nad F Y and Monceau P 1990 *J. Phys.: Condens. Matter* **2** 8327
[19] Sato H, Enoki T, Yamaura J and Yamamoto N 1999 *Phys. Rev.* B **59** 12836
[20] Carter M L and Withers R L 2005 *J. Solid State Chem.* **178** 1903
[21] Kanamori J 1959 *J. Phys. Chem. Solids* **10** 87
[22] Goodenough J B 1955 *Phys. Rev.* **100** 564